Precise Control of Lower Critical Solution Temperature of Thermosensitive Poly(2-isopropyl-2-oxazoline) via Gradient Copolymerization with 2-Ethyl-2-oxazoline as a Hydrophilic Comonomer

Joon-Sik Park[†] and Kazunori Kataoka*[,†,‡,§]

Department of Materials Engineering, Graduate School of Engineering, The University of Tokyo, 7-3-1 Hongo, Bunkyo-ku, Tokyo 113-8656, Japan; Center for Disease Biology and Integrative Medicine, Graduate School of Medicine, The University of Tokyo, Tokyo 113-0033, Japan; and Center for NanoBio Integration, The University of Tokyo, 7-3-1 Hongo, Bunkyo-ku, Tokyo 113-8656, Japan

Received March 13, 2006; Revised Manuscript Received June 23, 2006

ABSTRACT: The lower critical solution temperature (LCST) of amphiphilic poly(2-isopropyl-2-oxazoline) (P*i*PrOx) was precisely tuned via the copolymerization with 2-ethyl-2-oxazoline (EtOx) as a hydrophilic comonomer. The copolymerization was cationically initiated by methyl *p*-tosylate at the optimum condition (42 °C in acetonitrile) for living polymerization, obtaining the copolymers with a narrow molecular weight distribution ($M_w/M_n \leq 1.02$). The monomer reactivity ratios of 1.78 and 0.79 respectively were derived for EtOx and *i*PrOx from the cumulative and instantaneous compositions of the copolymers determined from the ^{1}H NMR and MALDI-TOF mass spectrometry. This set of the reactivity ratios are sufficiently different enough to form the gradient copolymers, in which each polymer chain has a trend of a gradually decreasing EtOx and an increasing *i*PrOx composition along the backbone from the α-terminal to ω-chain end. These gradient copolymers followed a rather simple rule in their thermosensitive behaviors to show a linear increase in LCST with an increasing mol % of EtOx. Consequently, a series of P(EtOx-*co*-*i*PrOx) with finely tuned LCST in aqueous medium were obtained through the cationic copolymerization simply by varying the initial composition of both monomers, opening a new way to engineer the thermosensitivity of polymeric materials directing to particular applications.

Introduction

Recently, enormous attention has been paid to so-called "smart" polymeric materials showing a discrete change in their propensity responding to external physical and chemical stimuli, including light, temperature, pH, and magnetic and electric fields. Of special interest is temperature-responsive polymers useful for various practical applications, such as supports for catalysts,[1] sensors,[2] separation systems,[3] enzymatic bioconjugates,[4] and drug carriers.[5] Drastic changes in solubility, turbidity, and other physicochemical properties of thermosensitive polymers can be simply induced by adding or removing heat energy, and such feasibility is particularly important to design "smart" polymeric materials that instantly respond to the external stimuli. Careful engineering of polymer structure should be needed for the fine-tuning of responding temperature as well as sharpness of transition. Furthermore, additional functionalization in a controllable manner may be required for some applications directing to construct thermosensitive block or graft copolymers, which have received growing interest particularly in bio-related fields.

In this regard, we have been recently focusing on the quantitative polymerization and selective end-functionalization of thermosensitive poly(2-isopropyl-2-oxazoline) (P*i*PrOx) telechelics.[6] The polymerization proceeded in a good controlled manner under an optimum temperature condition (42 °C) with appreciably narrow molecular weight distributions ($M_w/M_n \leq 1.03$), having never been accomplished in those of the conventional poly(2-oxazolines) (POx) homologues often viewed as "pseudopeptides".[7] Of importance is that P*i*PrOx exhibits a characteristic lower critical solution temperature (LCST) near physiological conditions, like poly(*N*-isopropylacrylamide) (PNIPAAm),[8] the typical representative of the thermosensitive polymers with numerous applications. The notable transition behaviors of P*i*PrOx, characterized by a fast responsivity, viz., transition sharpness, could be achieved by the precise control of the well-defined polymeric structures through the living polymerization mechanism. It should be also noted that POx, as a rule, are nontoxic and that some of them carry US Food and Drug Administration (FDA) approval.[9]

In the meantime, the LCST of P*i*PrOx can be controlled by incorporating the specific composition of hydrophilic or hydrophobic 2-oxazoline monomer units within the main chains, as in the case of conventional thermosensitive polymers.[10] A number of recent studies have shown that thermosensitive copolymers from different monomers are simply synthesized by the living ionic or controlled/living radical polymerization technique, and these copolymers with well-balanced hydrophilic/hydrophobic monomer sequences are attractive to realize the elaborate manipulability of their LCST values.[11] Nevertheless, little attention has been paid to the living cationic copolymerization between 2-isopropyl-2-oxazoline (*i*PrOx) and various hydrophilic/hydrophobic 2-substituted-2-oxazolines (Ox). Although there are several examples of copolymers composed of some Ox sequences including *i*PrOx,[12] the study on the LCST control of POx through the well-defined cationic copolymerization of *i*PrOx with either the hydrophilic or hydrophobic Ox comonomer has not been accomplished yet. Because there are various hydrophilic and hydrophobic Ox monomers, it is

[†] Graduate School of Engineering.
[‡] Graduate School of Medicine.
[§] Center for NanoBio Integration.
* To whom correspondence should be addressed: Tel +81-3-5841-7138; Fax +81-3-5841-7139; e-mail kataoka@bmw.t.u-tokyo.ac.jp.

10.1021/ma0605548 CCC: $33.50
Published on Web 08/22/2006

Scheme 1. Synthetic Scheme for the Gradient Copolymerization of 2-Ethyl-2-oxazoline (EtOx) and 2-Isopropyl-2-oxazoline (*i*PrOx) Initiated with Methyl *p*-Tosylate

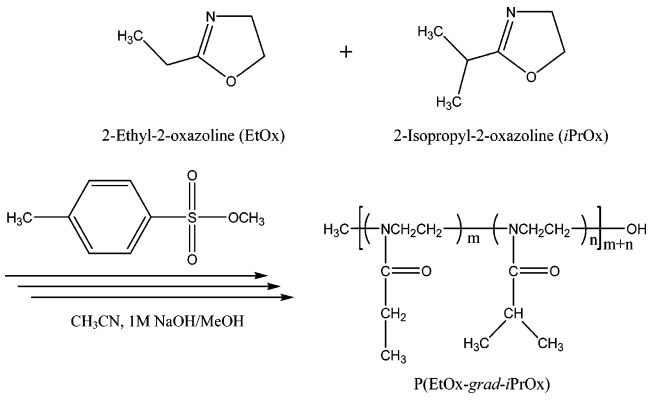

relatively easy to select the appropriate comonomer for varying the solubility of P*i*PrOx in water. However, careful consideration should also be taken into account for the diversity of the copolymerization conditions, derived from the many combinations among initiators, solvents, and temperatures vs the respective Ox monomers. It has been also noted that, in the controlled living copolymerization system of two monomers with sufficiently different reactivity ratios, a gradient copolymer, in which the instantaneous composition continuously varies along the chain contour, could be predominantly produced due to the feed composition drift that spontaneously occurs during the reaction.[13] Therefore, it was hypothesized that the choice of the appropriate hydrophilic or hydrophobic Ox comonomer exhibiting a sufficiently different reactivity against the *i*PrOx monomer may create thermosensitive gradient copolymers.

In the present study, we report the facile and precise synthetic route of thermosensitive gradient copolymers via the living cationic polymerization of *i*PrOx, including the specific composition of EtOx as a hydrophilic comonomer (Scheme 1). It was confirmed from the ^{1}H NMR and MALDI-TOF mass spectrometry that EtOx and *i*PrOx were found to have reactivity ratios sufficiently different from gradient copolymers under mild temperature conditions (42 °C). Furthermore, these POx gradient copolymers showed a rapid and linear response to temperature change from 38.7 to 67.3 °C.

Experimental Section

Materials. 2-Isopropyl-2-oxaxoline was synthesized from isobutyric acid (Wako Pure Chemical Industries, Ltd., Osaka, Japan) and 2-aminoethanol (Wako Pure Chemical Industries) as previously described.[6,14] Methyl *p*-tosylate (Tokyo Kasei Kogyo Co., Ltd., Tokyo, Japan) was distilled from calcium hydride under reduced pressure. 2-Ethyl-2-oxaxoline (Aldrich Chemical Co., Ltd., Milwaukee, WI) and acetonitrile (Wako Pure Chemical Industries) were distilled from calcium hydride following conventional procedures.[15] Other chemicals such as the 1 N NaOH aqueous solution and methanol were purchased from Wako Pure Chemical Industries and used without further purification.

Techniques. The ^{1}H NMR spectra were recorded using a JEOL EX 300 spectrometer at 300 MHz. The chemical shifts were reported in parts per million (ppm) downfield from tetramethylsilane. The molecular weights and molecular weight distributions were determined using a GPC (TOSOH HLC-8220) system equipped with two TSK gel columns ($G4000H_{HR}$ and $G3000H_{HR}$) and an internal refractive index (RI) detector. The columns were eluted with DMF containing lithium bromide (10 mM) and triethylamine (30 mM) at the flow rate of 0.8 mL/min and were maintained at a temperature of 40 °C. The molecular weights were calibrated using poly(ethylene glycol) (PEG) standards (Polymer Laboratories, Ltd., UK). The mass measurements were performed using a MALDI-TOF mass spectrometer (Bruker REFLEX III), operating at an acceleration voltage of 23 kV in the reflection mode. The UV−vis spectra were obtained using a V-550 UV/vis JASCO spectrophotometer.

Synthesis of Poly(2-isopropyl-2-oxazoline) (P*i*PrOx) Having a Hydroxyl Group at the ω-Terminal End. 2-Isopropyl-2-oxazoline (*i*PrOx) (10 g, 88.4 mmol) was added via a syringe to a solution of methyl *p*-tosylate (MeOTs) (0.186 g, 1.0 mmol) in acetonitrile (30 mL). The polymerization mixture was stirred at 42 °C for 476.5 h under an argon atmosphere. The mixture was cooled to room temperature and treated with methanolic NaOH (1 M) to introduce a hydroxyl group at one of the chain ends. The solution of Me-P*i*PrOx-OH was purified via dialysis for 2 days against distilled water and then recovered by lyophilization. Six samples were collected during the course of the polymerization. They were subjected to the same treatment above and analyzed by a MALDI-TOF mass spectrometer in order to determine the conversion yield (total yields: 9 g, 90%).

Synthesis of Poly(2-ethyl-2-oxazoline) (PEtOx) Having a Hydroxyl Group at the ω-Terminal End. 2-Ethyl-2-oxazoline (EtOx) (8.763 g, 88.4 mmol) was added via a syringe to a solution of MeOTs (0.186 g, 1.0 mmol) in acetonitrile (30 mL). The polymerization mixture was stirred at 42 °C for 315 h under an argon atmosphere. The mixture was then cooled to room temperature and treated with methanolic NaOH (1 M) to introduce a hydroxyl group at one of the chain ends. The solution of Me-PEtOx-OH was purified via dialysis for 2 days against distilled water and then recovered by lyophilization. Four samples were collected during the course of the polymerization. They were subjected to the same treatment described above and analyzed using a MALDI-TOF mass spectrometer in order to determine the conversion yield (total yields: 8.3 g, 95%).

Synthesis of Gradient Copolymers (P($EtOx_{25\%}$-*i*-$PrOx_{75\%}$), P($EtOx_{50\%}$-*i*-$PrOx_{50\%}$), P($EtOx_{75\%}$-*i*-$PrOx_{25\%}$)) Having a Hydroxyl Group at the ω-Terminal End. The respective mixtures of 2-ethyl-2-oxazoline ($EtOx_{25\%}$: 2.19 g, 22.1 mmol; $EtOx_{50\%}$: 4.38 g, 44.2 mmol; $EtOx_{75\%}$: 6.57 g, 66.3 mmol) and 2-isopropyl-2-oxazoline ($iPrOx_{75\%}$: 7.5 g, 66.3 mmol; $iPrOx_{50\%}$: 5 g, 44.2 mmol; $iPrOx_{25\%}$: 2.5 g, 22.1 mmol) were added to a solution of MeOTs (0.186 g, 1.0 mmol) in acetonitrile (30 mL). The polymerization mixture was stirred at 42 °C for 309.5 h (P($EtOx_{25\%}$-*i*-$PrOx_{75\%}$)), 407 h (P($EtOx_{50\%}$-*i*-$PrOx_{50\%}$)), and 288 h (P($EtOx_{75\%}$-*i*-$PrOx_{25\%}$)) under an argon atmosphere. The reaction mixtures were cooled to room temperature and then treated with methanolic NaOH (1 M) to introduce a hydroxyl group at one of the chain ends. The copolymer solutions were purified via dialysis for 2 days against distilled water and then recovered by lyophilization. Several samples of the respective copolymers were collected during the course of the copolymerization. They were subjected to the same treatment as described above and analyzed by MALDI-TOF mass and ^{1}H NMR spectrometers in order to determine the conversion yield and composition of the copolymers (total yields: 8.4 g, 87% (P($EtOx_{25\%}$-*i*-$PrOx_{75\%}$)), 8.5 g, 91% (P($EtOx_{50\%}$-*i*-$PrOx_{50\%}$)), 7.7 g, 85% (P($EtOx_{75\%}$-*i*-$PrOx_{25\%}$)).

MALDI-TOF Mass Spectrometry. An external calibration was performed using poly(ethylene glycol) standards (MeO-PEG-OH; MW = 5000, 12 000, NOF Corp). Ions were generated by laser desorption at 337 nm (N_2 laser, 3 ns pulse width, 10^6-10^7 W/cm^2). For each spectrum, ~400 transients were accumulated and all spectra were recorded in the reflection mode. The data evaluation was performed with the Bruker XMASS program using the reflection spectra only in order to achieve a better signal-to-noise ratio. α-Cyano-4-hydroxycinnamic acid (CCA) (Fluka) was selected as a suitable matrix. A trifluoroacetic acid/acetonitrile (0.1% TFA: CH_3CN = 2:1) solution of CCA (10 mg/mL) was mixed with a solution of the polymer in acetonitrile (1 mg/mL) at an equimolar ratio. The resulting mixture was shaken for a few seconds. An aliquot of the mixture (1 μL) was placed on the target plate and inserted into the ion source chamber after being slowly dried. The polymer concentration of the polymer/matrix mixture solution could

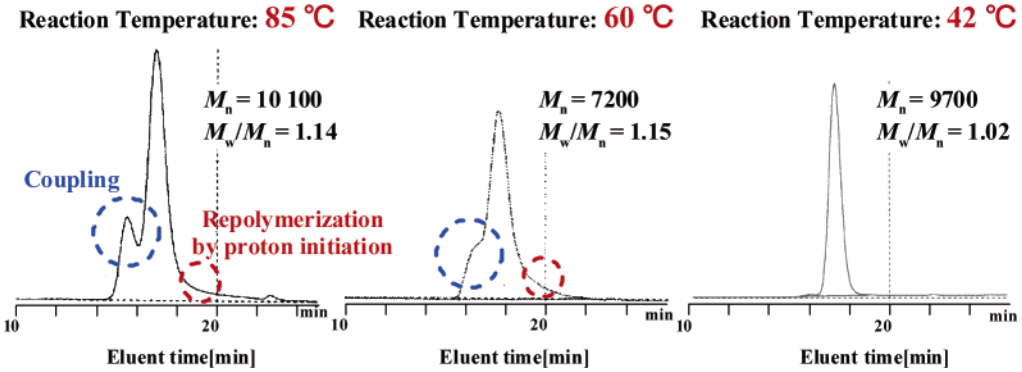

Figure 1. GPC diagrams of P*i*PrOx (DP_{theo} = 88.4) synthesized under different temperature conditions (PEG standard, eluent: DMF (containing 10 mM LiCl and 30 mM TEA), temperature: 40 °C, RI detection).

Table 1. Copolymerization Results of *i*PrOx with EtOx at Different Feed Composition[a] and Their T_{cp} Values

feed ratio (EtOx:*i*PrOx)	yield (%)	M_n (M_w/M_n) MALDI-TOF-MS[b]	M_n (M_w/M_n) GPC[c]	*m*:*n*[d]	T_{cp}[e] (°C) (with 150 mM NaCl)
100:0	95	8300 (1.01)	8000 (1.02)	100:0	
25:75	87	8700 (1.01)	9300 (1.02)	22:78	67.3 (65.4)
50:50	91	9300 (1.01)	9300 (1.02)	48:52	55.2 (54.0)
75:25	85	9100 (1.01)	9300 (1.02)	73:27	46.0 (45.1)
0:100	90	10200 (1.01)	9700 (1.02)	0:100	38.7 (37.4)

[a] Reaction conditions: ([EtOx] + [*i*PrOx])/$[MeOTs]_{init}$ = 88.4, $[MeOTs]_{init}/[CH_3CN]_{solv}$ = 0.033 mol/L, 42 °C, terminated with methanolic NaOH (1 M) for hydroxyl ω-end group. [b] Bruker REFLEX III, operating at an acceleration voltage of 23 kV in the reflector mode. [c] DMF (10 mM LiCl and 30 mM TEA), 40 °C, RI detection. [d] Determined by ^{1}H NMR spectroscopy for the final copolymer products (monomer composition: *m* = [EtOx], *n* = [*i*PrOx]). [e] Measured by UV−vis spectroscopy (*c* = 1.0 wt %).

be diluted for the optimum ionization with an acetone solution of CCA (10 mg/mL).

Turbidity Measurements. Cloud points were determined by spectrophotometric detection of the changes in transmittance (λ = 500 nm) of the aqueous polymer solutions (1.0 wt %) heated at a constant rate (0.5 °C/min). The samples were placed in a temperature-controlled circulating water bath. Values for the cloud points of the polymer solutions were determined as the temperature corresponding to a 10% decrease in optical transmittance.

Results and Discussion

Synthesis of Homopolymers. Prior to the synthesis of copolymers, the respective polymerization behaviors of both the P*i*PrOx and PEtOx homopolymers needed to be screened in order to gain the kinetic information under the identical reaction conditions.

As far as the polymerization of *i*PrOx initiated with methyl *p*-tosylate (MeOTs) in acetonitrile, the mild temperature condition should be adapted for avoiding the spontaneously occurring side reactions such as chain transfer and coupling, resulting in wide molecular weight distributions (Figure 1). There has been an argument that the branching in 2-alkyl-2-oxazoline polymerization is susceptible to occur with the increasing monomer conversion, deriving from a chain transfer to monomer followed by repolymerization and coupling.[16] This effect was visible in the GPC traces of Figure 1 as a lower molecular weight tailing and a higher molecular weight shoulder, even notable with increasing temperature. In particular, at polymerization temperature of 85 °C, the higher molecular weight shoulder on the GPC diagram become pronounced, which is most likely due to the occurrence of a coupling or branching. In the chain transfer step, a monomer, instead of adding nucleophilically to the growing chain end, abstracts a proton to produce a dormant enamine-terminated polymer chain and an oxazolinium monomer which can continue the kinetic chain. In the coupling (or branching) step, after the majority of the presumably more

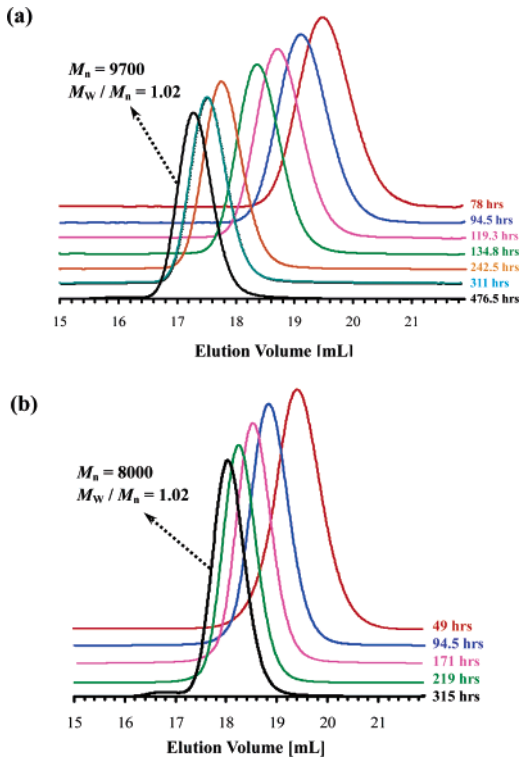

Figure 2. GPC traces of two homopolymers ((a) P*i*PrOx and (b) PEtOx) having different molecular weights (PEG standard, eluent: DMF (containing 10 mM LiCl and 30 mM TEA), temperature: 40 °C, RI detection).

reactive oxazoline monomer is exhausted, the terminal enamine end groups on the dormant chains are able to compete for the oxazolinium chain ends. Each of these couplings produces a branch point and regenerates another oxazolinium end group. The evidence of these side reactions was often observed as both lower molecular weight tailings and higher molecular weight shoulders in the GPC traces of P*i*PrOx, so that the mild

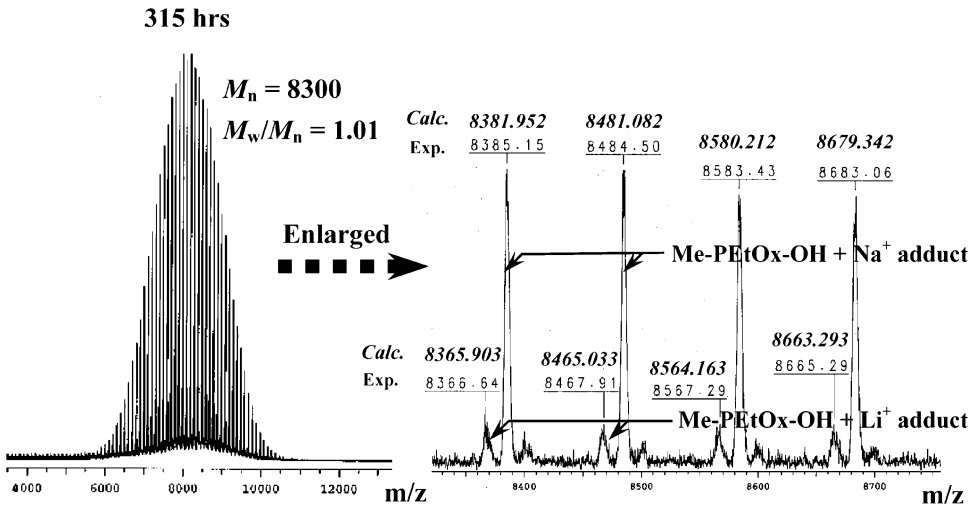

Figure 3. MALDI-TOF mass spectrum of ω-hydroxyl-terminated PEtOx after 315 h (left) and its expanded spectrum in the region of 8330−8750 (right).

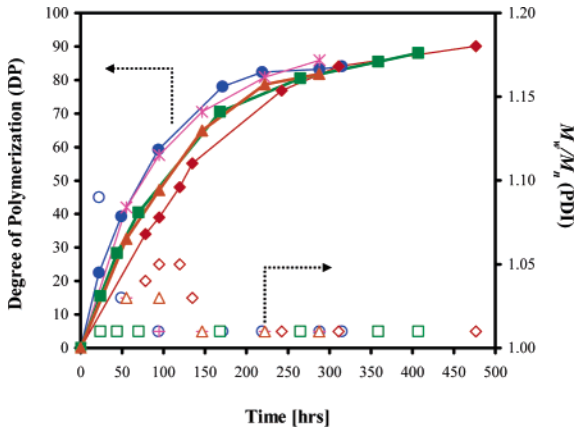

Figure 4. Degree of polymerization (DP) (closed symbols) and polydispersity index (PDI) (open symbols), obtained from MALDI-TOF mass spectrometry, against reaction time for two homopolymers (P*i*PrOx (◆, ◇) and PEtOx (●, ○)) and three gradient copolymers (P($EtOx_{25\%}$*i*$PrOx_{75\%}$) (▲, △), P($EtOx_{50\%}$*i*$PrOx_{50\%}$) (■, □), and P($EtOx_{75\%}$*i*$PrOx_{25\%}$) (*, +)).

temperature of 42 °C was found to be a key condition factor to have complete control over the side reactions (Figure 1).

Based on the results described above, the cationic ring-opening polymerization of *i*PrOx initiated with MeOTs was done to obtain the well-defined poly(2-isopropyl-2-oxazoline) carrying a hydroxyl group at one end (Me-P*i*PrOx-OH). Under mild temperature conditions (42 °C), the polymerization had to be left to proceed for lengths of time up to ca. 476.5 h, but no noticeable side reactions occurred. It was ascertained from the GPC diagrams (Figure 2a) and MALDI-TOF mass spectra (Figure S1a−g in the Supporting Information) that the time-dependent change in the number-average molecular weight (M_n) and the molecular weight distribution were consistent with the living polymerization process; the polydispersity index was low (PDI_{GPC} = 1.02, PDI_{TOF-MS} = 1.01), and the experimental M_n value ($M_{n,GPC}$ = 9700, $M_{n,TOF-MS}$ = 10 200) was close to the value predicted from the initial monomer/initiator ratio ($M_{n,calc}$ = 10 000) (Table 1). An end-group analysis of the polymer was also performed from the MALDI-TOF mass spectrum recorded for a Me-P*i*PrOx-OH after 476.5 h (Figure S1g in the Supporting Information). The most intense signal can be assigned to the sodium adduct of Me-P*i*PrOx-OH, while the second most intense signal is due to the potassium adduct of Me-P*i*PrOx-OH.

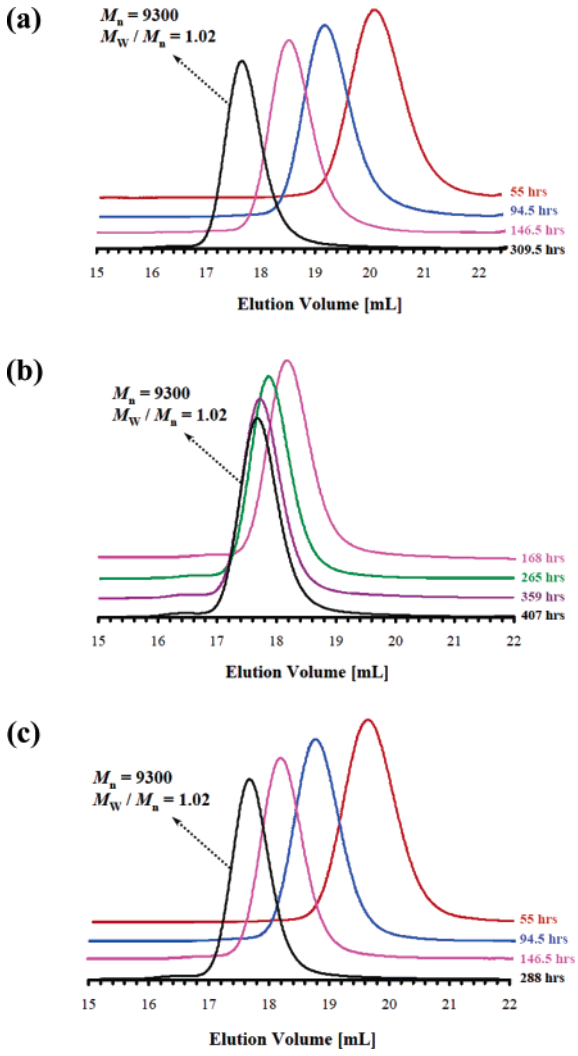

Figure 5. GPC traces of three gradient copolymers ((a) P($EtOx_{25\%}$*i*$PrOx_{75\%}$), (b) P($EtOx_{50\%}$*i*$PrOx_{50\%}$), and (c) P($EtOx_{75\%}$*i*$PrOx_{25\%}$)) having different molecular weights (PEG standard, eluent: DMF (containing 10 mM LiCl and 30 mM TEA), temperature: 40 °C, RI detection).

The polymerization of Me-PEtOx-OH (8.763 g, 88.4 mmol) was also done under the synthetic conditions similar to that of Me-P*i*PrOx-OH with the initiation of methyl *p*-tosylate (MeOTs) (0.186 g, 1.0 mmol) in acetonitrile (30 mL) under mild temperature conditions (42 °C), followed by the treatment with

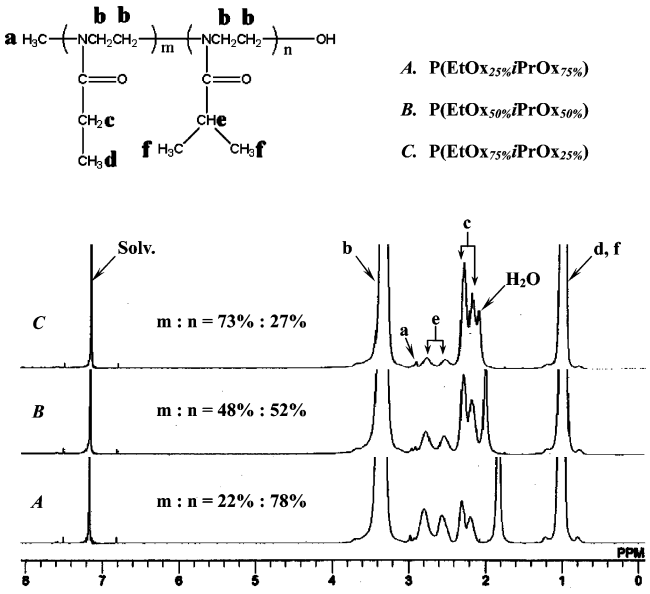

Figure 6. ^{1}H NMR spectra for the final products of three gradient copolymers (P(EtOx$_{25\%}$*i*PrOx$_{75\%}$), P(EtOx$_{50\%}$*i*PrOx$_{50\%}$), and P(EtOx$_{75\%}$*i*PrOx$_{25\%}$)) in $CDCl_3$ at 25 °C.

methanolic NaOH (1 M) for introducing a hydroxyl ω-end group. Under this condition, the polymerization should be left to proceed for ca. 315 h, but no noticeable side reactions occurred, as in the system of Me-P*i*PrOx-OH. It was confirmed from the GPC diagrams (Figure 2b) and MALDI-TOF mass spectra (Figure S2a−d) in the Supporting Information and Figure 3) that the polydispersity indices of all the sampling polymers including the final product were below 1.03, and the experimental M_n value ($M_{n,GPC}$ = 8000, $M_{n,TOF-MS}$ = 8300) was almost identical to the value predicted from the initial monomer/initiator ratio ($M_{n,calc}$ = 8800) (Table 1). The end-group analysis of the Me-PEtOx-OH was also done using the MALDI-TOF mass spectrum recorded after 315 h (Figure 3). The most intense signal can be assigned to the sodium adduct of Me-PEtOx-OH, while the second most intense signal is due to the lithium adduct of Me-PEtOx-OH. The ^{1}H NMR spectrum of Me-PEtOx-OH in $CDCl_3$ presented a broad singlet at 3.4 ppm attributed to the methylene protons of the polymer backbone, two broad singlets at 2.1−2.4 ppm, ascribed to methylene protons of the ethyl side chain and a broad singlet at 1.0 ppm due to the side chain methyl protons (Figure S3). To the best of our knowledge, this is the first demonstration of polymerizing an extremely monodispersive PEtOx homopolymers ($M_w/M_n \leq 1.02$) without inadvertent side reactions such as chain transfer and coupling,[16] often observed during the synthesis of conventional PEtOx systems under high-temperature conditions.[17]

The time-dependent monomer conversion obtained from the MALDI-TOF mass spectrometry for the respective polymerizations of both *i*PrOx and EtOx is also depicted in Figure 4, whereby the degree of polymerization (DP) was positioned at the left ordinate and the polydispersity index (PDI) (M_w/M_n) at the right ordinate. From the time-dependent DP and PDI changes of the two respective homopolymers, it was obvious that the polymerization rate of EtOx (●) was somewhat faster than that of *i*PrOx (◆) at 42 °C.

Synthesis of Gradient Copolymers. In view of the synthesis result of the two homopolymers described above, we planned to next synthesize a series of copolymers comprising EtOx and *i*PrOx in order to explore the hydrophilic contribution of EtOx on the LCST of P*i*PrOx (Scheme 1). The respective mixtures of 2-ethyl-2-oxazoline (EtOx$_{25\%}$: 2.19 g, 22.1 mmol; EtOx$_{50\%}$: 4.38 g, 44.2 mmol; EtOx$_{75\%}$: 6.57 g, 66.3 mmol) and 2-isopropyl-2-oxazoline (*i*PrOx$_{75\%}$: 7.5 g, 66.3 mmol; *i*PrOx$_{50\%}$: 5 g, 44.2 mmol; *i*PrOx$_{25\%}$: 2.5 g, 22.1 mmol) were added to a solution of MeOTs (0.186 g, 1.0 mmol) in acetonitrile (30 mL) and polymerized at 42 °C, as in the case of the two homopolymers (PEtOx and P*i*PrOx). The synthesis results of three copolymers (P(EtOx$_{25\%}$*i*PrOx$_{75\%}$), P(EtOx$_{50\%}$*i*PrOx$_{50\%}$), and P(EtOx$_{75\%}$*i*PrOx$_{25\%}$)) including two homopolymers with the same initial monomer/initiator ratio (DP_{calc} = 88.4) are summarized in Table 1. The polymerization behaviors of the copolymers with the initial EtOx and *i*PrOx molar ratios of 25%:75%, 50%:50%, and 75%:25% were characterized by the time-dependent change in the DP and PDI via the MALDI-TOF mass and GPC traces, as seen in Figure 4. Regardless of the comonomer ratio in the feed, the experimental degree of polymerization (DP from MALDI-TOF mass spectrometry) of the respective copolymers was close to the predicted value from the initial monomer/initiator ratio (DP_{calc} = 88.4) and their

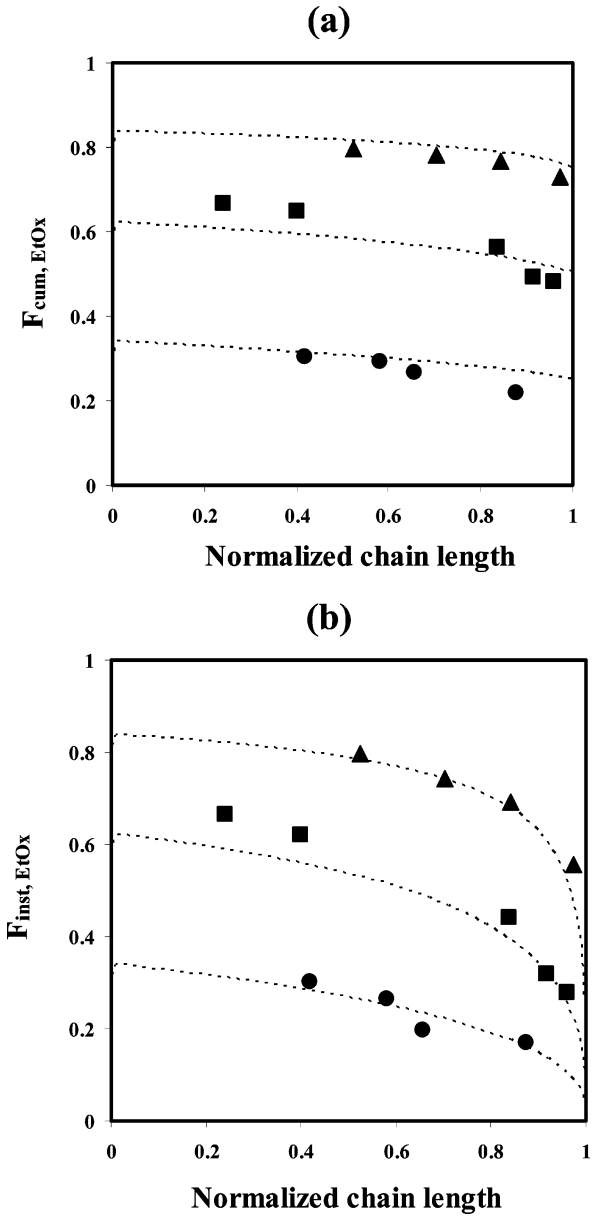

Figure 7. (a) Cumulative ($F_{cum,EtOx}$) and (b) instantaneous ($F_{inst,EtOx}$) composition plots for spontaneous gradient copolymers. The theoretical prediction curves (dotted) were calculated using the simulation program PROCOP[20] (P(EtOx$_{25\%}$*i*PrOx$_{75\%}$) (●), P(EtOx$_{50\%}$*i*PrOx$_{50\%}$) (■), and P(EtOx$_{75\%}$*i*PrOx$_{25\%}$) (▲)).

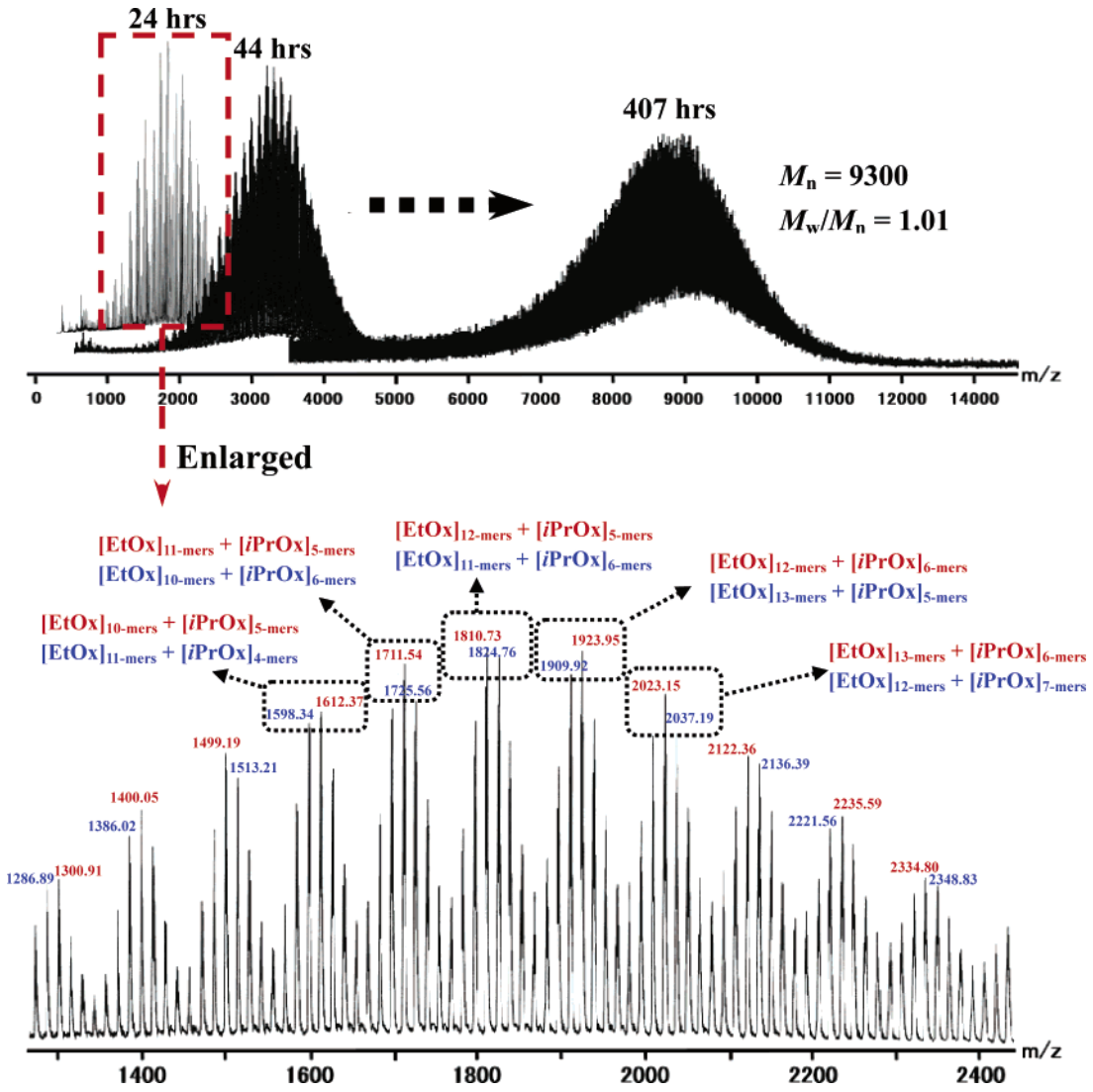

Figure 8. MALDI-TOF mass spectra of gradient copolymer samples comprising $EtOx_{50\%}$ and $iPrOx_{50\%}$ after 24, 44, and 407 h, respectively (upper), and enlarged detail in the mass region of 1300−2400 for the first sampling P($EtOx_{50\%}$-*i*-$PrOx_{50\%}$) after 24 h (lower).

molecular weight distributions were appreciably narrow in all cases (Figure 4). The GPC traces of the three copolymers with different monomer ratios in the feed (P($EtOx_{25\%}$-*i*-$PrOx_{75\%}$), P($EtOx_{50\%}$-*i*-$PrOx_{50\%}$), and P($EtOx_{75\%}$-*i*-$PrOx_{25\%}$)), which were sampled at different polymerization times, also showed an increase in the molar mass with time and symmetrical monomodal peaks, as shown in Figure 5a−c. In addition, the compositions of the final copolymer products determined by ^{1}H NMR spectrometry were in good agreement with the calculated values from the feed ratio of both monomers, indicating their quantitative conversion into the respective copolymers (Figure 6 and Table 1).

In this living polymerization system, copolymers are expected to have a gradient composition, providing sufficiently different reactivity ratios of the two monomers, EtOx and *i*PrOx. Indeed, from the composition analysis by ^{1}H NMR spectrometry of the respective copolymer samplings (monomer conversions: ca. 20%−40%) plotted in Figure 4, the reactivity ratios of the respective monomers were calculated to be $r_{EtOx} = 1.78$ and $r_{iPrOx} = 0.79$ through the nonlinear Tidwell−Mortimer (TM) method, showing the most reasonable result among the well-established calculation methods for the further composition analysis of the copolymers (For the details on the determination of the reactivity ratios, see Tables S1 and S2 in the Supporting Information.) While in a conventional process the monomer reactivity ratios can be measured at low conversion (≤ca. 10%) with different monomer feeds, in the living process high polymer is not formed immediately in the reaction. Besides, measurements at such a low conversion could be also affected by the different reactivity of the initiator against a specific monomer. For this reason, the reactivity ratios should be calculated at comparatively higher monomer conversions (20% or higher).[13,18] As far as the polymerization of 2-oxazolines is concerned, it is also well-known that the initial polymerization rate can be different from the terminal polymerization rate,[19] so that we selected monomer conversions of ca. 20%−40% as a reasonable interval in this living system. This difference in the reactivity ratios of two monomers indicates that EtOx should initially be consumed much faster than *i*PrOx. However, because of the decreasing concentration of the former in the residual feed, the rate of its incorporation into the polymer chain also decreased. This resulted in an increased instantaneous incorporation of *i*PrOx into the copolymer as the reaction progressed and ultimately in the formation of an *i*PrOx-rich chain end. Because of the simultaneous initiation and uniform propagation kinetics in this living system as known from the appreciably low polydispersity indices ($M_w/M_n \leq 1.02$), each polymer chain should display a similar trend of a gradually decreasing EtOx and an increasing *i*PrOx composition along the backbone from the α-terminal to active ω-chain end. The cumulative and

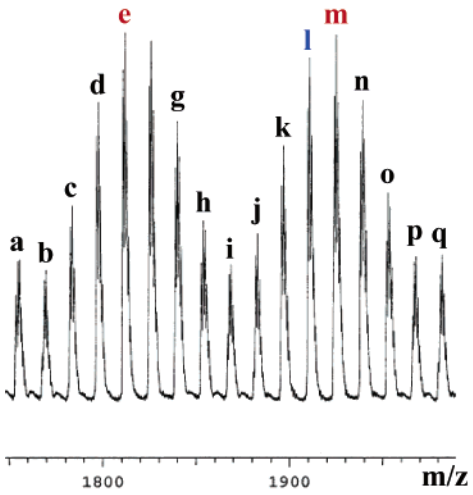

Assign.	$Mass_{calc.}$	$Mass_{exp.}$
a. $[EtOx]_{16\text{-mers}} + [iPrOx]_{1\text{-mers}}$	1754.270	1754.62
b. $[EtOx]_{15\text{-mers}} + [iPrOx]_{2\text{-mers}}$	1768.298	1768.65
c. $[EtOx]_{14\text{-mers}} + [iPrOx]_{3\text{-mers}}$	1782.326	1782.65
d. $[EtOx]_{13\text{-mers}} + [iPrOx]_{4\text{-mers}}$	1796.354	1796.69
e. $[EtOx]_{12\text{-mers}} + [iPrOx]_{5\text{-mers}}$	1810.382	1810.73
f. $[EtOx]_{11\text{-mers}} + [iPrOx]_{6\text{-mers}}$	1824.410	1824.76
g. $[EtOx]_{10\text{-mers}} + [iPrOx]_{7\text{-mers}}$	1838.438	1838.79
h. $[EtOx]_{9\text{-mers}} + [iPrOx]_{8\text{-mers}}$	1852.466	1852.83
i. $[EtOx]_{16\text{-mers}} + [iPrOx]_{2\text{-mers}}$	1867.428	1867.84
j. $[EtOx]_{15\text{-mers}} + [iPrOx]_{3\text{-mers}}$	1881.456	1881.87
k. $[EtOx]_{14\text{-mers}} + [iPrOx]_{4\text{-mers}}$	1895.484	1895.88
l. $[EtOx]_{13\text{-mers}} + [iPrOx]_{5\text{-mers}}$	1909.512	1909.92
m. $[EtOx]_{12\text{-mers}} + [iPrOx]_{6\text{-mers}}$	1923.540	1923.95
n. $[EtOx]_{11\text{-mers}} + [iPrOx]_{7\text{-mers}}$	1937.568	1937.99
o. $[EtOx]_{10\text{-mers}} + [iPrOx]_{8\text{-mers}}$	1951.596	1952.02
p. $[EtOx]_{9\text{-mers}} + [iPrOx]_{9\text{-mers}}$	1965.624	1966.05
q. $[EtOx]_{16\text{-mers}} + [iPrOx]_{3\text{-mers}}$	1980.586	1981.07

Figure 9. Enlarged detail of MALDI-TOF mass spectrum in the region of 1750−1990 (m/z) for gradient copolymer sample comprising $EtOx_{50\%}$ and $iPrOx_{50\%}$ after 24 h (left) and assignment of mass spectral peaks (right).

instantaneous composition plots ($F_{cum,EtOx}$ and $F_{inst,EtOx}$, respectively) vs the normalized chain length were obtained for the three copolymerizations with different initial molar ratios of EtOx and *i*PrOx in the feed (Figure 7). According to the plots, the shape of the obtained gradient copolymers closely followed the theoretical predictions using $r_{EtOx} = 1.78$ and $r_{iPrOx} = 0.79$.[20] In particular, the plots of the instantaneous composition vs normalized chain length showed the dependence of the gradient shapes on the initial feed composition. When the initial feed ratio of EtOx and *i*PrOx was varied from 75%:25% to 25%:75%, no significant continuous change in the instantaneous composition was observed, suggesting the gentle slope of the gradient along the copolymer main chain. The feasibility of this type of methodology has been well-known to trace the composition drift of gradient copolymers in the example of atom transfer radical polymerization (ATRP) living system.[13]

In addition, a series of MALDI-TOF mass spectra for $P(EtOx_{50\%}iPrOx_{50\%})$, which were sampled at different polymerization times, were obtained as shown in Figure 8, showing a good coincidence with the results of the GPC traces. When viewing the copolymers by mass spectra, the relative abundance of all the copolymers with a defined chain length reflects the information about the sequence and composition present in the copolymer.[21] The MALDI-TOF mass spectrometry thus provided a useful method to evaluate these two quantities with good precision, comparing the theoretical mass values and relative intensities for a specific copolymer with the experimental mass spectrum. The series of all the copolymer samplings with the chain lengths below ca. $M_n = 10\,000$ could provide comparatively clearer mass spectra, and the enlarged mass spectrum of $P(EtOx_{50\%}iPrOx_{50\%})$ sampled after 24 h was selected for the detailed analysis of copolymer composition and sequence distribution (Figure 8). All the peaks shown in the mass spectrum of Figure 8 were assigned to copolymers comprised of the EtOx and *i*PrOx monomer units with both methyl groups at the α-terminals and hydroxyl groups at the ω-terminals. The calculated mass of each copolymer is expressed by the following equation:

$$\begin{aligned} \text{mass}_{\text{calc}} &= [\text{EtOx}]_{m-\text{mers}} + [i\text{PrOx}]_{n-\text{mers}} \\ &= \Delta[\text{EtOx}]_m + \Delta[i\text{PrOx}]_n + \\ &[\alpha\text{-methyl and } \omega\text{-hydroxyl groups}] + [\text{Na}^+] \end{aligned}$$

where $\text{mass}_{\text{calc}}$ (m/z) is the calculated mass of a copolymer with degree of polymerization nearest the measured value, Δ[EtOx] (or Δ[*i*PrOx]) is the mass of the monomer unit, and $[Na^+]$ is the mass of a sodium ion. The detailed peak assignments are summarized in Table 2, where mass_{exp} is the experimental mass value of the most and second intense signals among the respective homologue series in the mass region of 1300−2400. For instance, the strongest signal ($\text{mass}_{\text{exp}} = 1810.73$) and second most intense signal ($\text{mass}_{\text{exp}} = 1824.76$) in the mass region of 1750−1990 were in good agreement with the calculated mass values of the two corresponding copolymers, as shown below.

$$[\text{EtOx}]_{12-\text{mers}} + [i\text{PrOx}]_{5-\text{mers}} = 99.13 \times 12 + 113.158 \times 5 + 32.042 + 22.99 = 1810.382$$

$$[\text{EtOx}]_{11-\text{mers}} + [i\text{PrOx}]_{6-\text{mers}} = 99.13 \times 11 + 113.158 \times 6 + 32.042 + 22.99 = 1824.410$$

A more detailed assignment for all the mass spectral peaks in the region of 1750−1990 is also presented in Figure 9. Similar results for the other two gradient copolymers ($P(EtOx_{25\%}iPrOx_{75\%})$ and $P(EtOx_{75\%}iPrOx_{25\%})$) with different monomer ratios in the feed were also confirmed by MALDI-TOF mass spectrometry (Figures S4a−d and S5a−d in the Supporting Information).

In the case that the MALDI-TOF mass spectra were clearly recognized, the contour map exhibiting the number of *i*PrOx units per chain on the abscissa and the number of EtOx units per chain on the ordinate could be obtained by 2D plots using

Table 2. Assignment of MALDI-TOF Mass Spectral Peaks Shown in Figure 8

assignt	$mass_{calc}$	$mass_{exp}$	assignt	$mass_{calc}$	$mass_{exp}$
$[EtOx]_{8-mers} + [iPrOx]_{4-mers}$	1300.704	1300.91	$[EtOx]_{9-mers} + [iPrOx]_{3-mers}$	1286.676	1286.89
$[EtOx]_{9-mers} + [iPrOx]_{4-mers}$	1399.834	1400.05	$[EtOx]_{10-mers} + [iPrOx]_{3-mers}$	1385.806	1386.02
$[EtOx]_{10-mers} + [iPrOx]_{4-mers}$	1498.964	1499.19	$[EtOx]_{9-mers} + [iPrOx]_{5-mers}$	1512.992	1513.21
$[EtOx]_{10-mers} + [iPrOx]_{5-mers}$	1612.122	1612.37	$[EtOx]_{11-mers} + [iPrOx]_{4-mers}$	1598.094	1598.34
$[EtOx]_{11-mers} + [iPrOx]_{5-mers}$	1711.252	1711.54	$[EtOx]_{10-mers} + [iPrOx]_{6-mers}$	1725.280	1725.56
$[EtOx]_{12-mers} + [iPrOx]_{5-mers}$	1810.382	1810.73	$[EtOx]_{11-mers} + [iPrOx]_{6-mers}$	1824.410	1824.76
$[EtOx]_{12-mers} + [iPrOx]_{6-mers}$	1923.540	1923.95	$[EtOx]_{13-mers} + [iPrOx]_{5-mers}$	1909.512	1909.92
$[EtOx]_{13-mers} + [iPrOx]_{6-mers}$	2022.670	2023.15	$[EtOx]_{12-mers} + [iPrOx]_{7-mers}$	2036.698	2037.19
$[EtOx]_{14-mers} + [iPrOx]_{6-mers}$	2121.800	2122.36	$[EtOx]_{13-mers} + [iPrOx]_{7-mers}$	2135.828	2136.39
$[EtOx]_{14-mers} + [iPrOx]_{7-mers}$	2234.958	2235.59	$[EtOx]_{15-mers} + [iPrOx]_{9-mers}$	2220.930	2221.56
$[EtOx]_{15-mers} + [iPrOx]_{7-mers}$	2334.088	2334.80	$[EtOx]_{14-mers} + [iPrOx]_{8-mers}$	2348.116	2348.83

Microsoft Excel 2002 software.[22] After completing the precise mass assignment of all the peaks in the region of 1300−2400 (m/z) for the P($EtOx_{50\%}iPrOx_{50\%}$) sampling after 24 h, the contribution of each monomer unit to the calculated mass value of a copolymer with the degree of polymerization to nearest the measured value was determined, and the relative abundance (or intensity) of the assigned copolymer was represented as a function of the number of EtOx and *i*PrOx units (Figure 10a). From this 2D graph, it was obvious that the amount of EtOx in the copolymer backbone was ca. twice that of *i*PrOx during the initial period of copolymerization (24 h), which was caused by the sufficiently different reactivity ratios of the two monomers. Furthermore, the six contour maps after 24, 44, 70, 168, 265, and 407 h are also represented on the single $x-y$ coordinate system with the similar treatments (Figure 10b). Since it was hard to consider all the mass regions of the copolymer, the specific intervals within the seven lines and seven columns centering on the most intense signals should be selectively exhibited for clarification. The traces of all the contour maps were in good agreement with the result of the composition analysis of the two monomer units by ^{1}H NMR spectrometry as shown in Figure S6 of the Supporting Information.

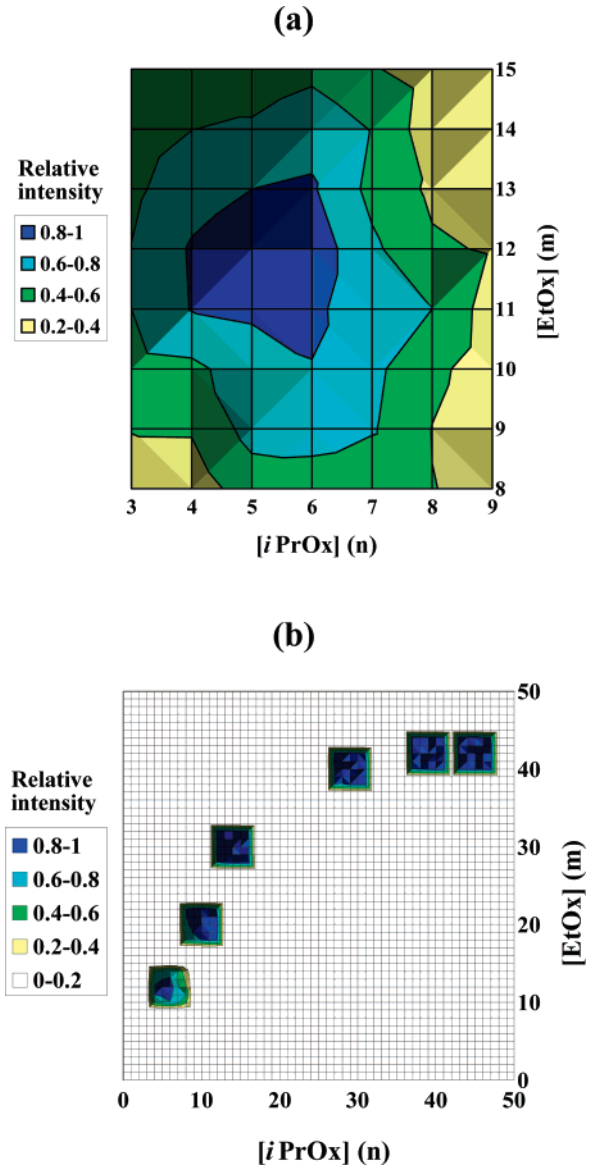

Figure 10. Gradient copolymer fingerprint obtained from MALDI-TOF mass analysis: a contour map showing the number of *i*PrOx units on the abscissa and the number of EtOx units on the ordinate (a) in the mass region of 1300−2400 for the first sampling P($EtOx_{50\%}iPrOx_{50\%}$) after 24 h and (b) trace of six contour maps obtained after 24, 44, 70, 168, 265, and 407 h.

Determination of the Cloud Points (T_{cp}). The measurement of the changing points in turbidity, defined here as the cloud points (T_{cp}), was adapted to determine the lower critical solution temperature (LCST) of a polymer solution. Figure 11a shows the dependence of the turbidity on the increasing temperature for the (co)polymer solutions with a different EtOx composition. The transmittance sharply decreased at a specific temperature in phosphate-buffered solution (10 mM PBS (pH = 7.4)) in

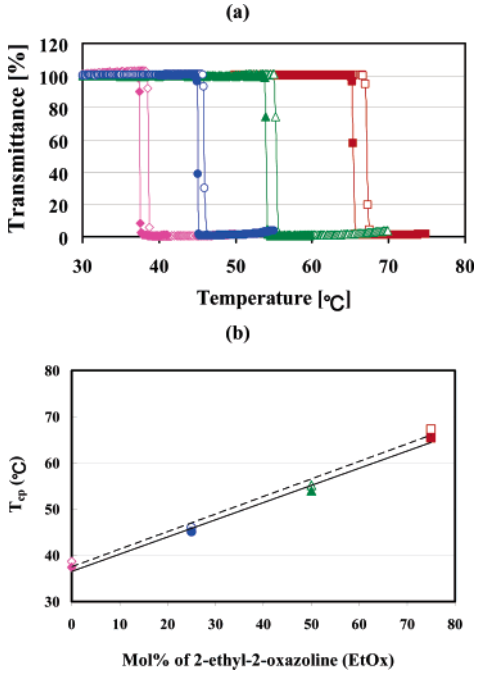

Figure 11. (a) Transmittance changes at 500 nm of 1.0 wt % (co)-polymer solutions (P*i*PrOx (◆, ◇), P($EtOx_{25\%}iPrOx_{75\%}$) (●, ○), P($EtOx_{50\%}iPrOx_{50\%}$) (▲, △), and P($EtOx_{75\%}iPrOx_{25\%}$) (■, □)) as a function of temperature (10 mM PBS (pH = 7.4) in the absence (open shape) or presence (closed shape) of 150 mM NaCl, rate 0.5 °C/min). (b) Relationship between cloud point (T_{cp}) and comonomer (EtOx) composition in the (co)polymers.

the absence (open symbols) or presence (closed symbols) of 150 mM NaCl, indicating a sharp LCST-type phase transition. The LCST values were found to linearly increase with the increasing mol % of EtOx (*n*), from 38.7 °C (or 37.4 °C) at $n = 0\%$ to 67.3 °C (or 65.4 °C) at $n = 75\%$ for a 1.0 wt % polymer solution in the absence (or presence) of 150 mM NaCl (Figure 11b). Regardless of the *i*PrOx to EtOx ratio, an exceedingly clear sensitivity of the phase separation was observed in all cases, whereas no change in transmittance appeared in the case of a PEtOx homopolymer at the measured temperatures up to 90 °C (Table 1). It was also observed that the LCST values of the (co)polymer solutions in the presence of 150 mM NaCl, viz., near the physiological condition, slightly shifted to lower temperatures in all cases compared to that in the absence of NaCl. This result was in agreement with the well-known "salting-out" effect of NaCl.[23]

A notable point of these turbidity results is that observed transition was appreciably sharp and simply correlated with the ratio of both monomers in the copolymers even though they have the compositional gradient along the polymer strand. It may be reasonable to assume that the LCST property of such a gradient copolymer may become complicated due to a possible formation of micelle-like molecular association derived from a deviating amphiphilicity along the polymer chain. Nevertheless, the static light scattering (SLS) measurements of the solution with varying temperature provided no obvious sign of assembly formation, keeping the weak and constant scattering intensity up to the LCST (data not shown). Although we may not exclude the possibility of conformational change in a single strand of the gradient copolymers below LCST due to the deviating amphiphilicity in the strand, turbidity behavior follows a rather simple and practical rule to be correlated with the ratio of both monomers in the copolymers. Detailed solution behavior of these gradient copolymers should be an important topic for the further study to understand their actual molecular dynamics related to temperature change, yet the present study recalls the well-established oxazoline polymerization as a convenient procedure to obtain the copolymers with extremely narrow molecular weight distribution and finely tuned LCST.

Conclusions

This study developed the facile and precise synthetic route of thermosensitive POx gradient copolymers via the living cationic polymerization of 2-isopropyl-2-oxazoline (*i*PrOx) mixed with a specific composition of 2-ethyl-2-oxazoline (EtOx) as a hydrophilic comonomer. The oxazoline monomers (EtOx and *i*PrOx) had sufficiently different reactivity ratios of 1.78 and 0.79, respectively, leading to obtain the gradient copolymers with varying composition and very narrow molecular weight distribution. Turbidity measurements revealed that LCST of the gradient copolymers can be minutely modulated over a broad range of temperature from 38.7 to 67.3 °C simply by varying the molar ratio of EtOx to *i*PrOx. This approach of copolymerizing a variety of oxazoline monomers with different hydrophobic and hydrophilic balance, in a condition to attain living polymerization (mild temperature in acetonitrile), apparently lead to the systematic preparation of versatile end-functionalized polyoxazoline derivatives with finely tuned LCST, which have a promising feasibility particularly in biomedical applications as constructing thermosensitive bioconjugates and drug delivery systems.

Acknowledgment. This work was financially supported by Special Coordination Funds for Science and Technology from the Ministry of Education, Culture, Sports, Science and Technology of Japan (MEXT) as well as by the Core Research for Evolutional Science and Technology (CREST) from the Japan Science and Technology Agency (JST).

Supporting Information Available: Figures S1−S6 and Tables S1 and S2. This material is available free of charge via the Internet at http://pubs.acs.org.

References and Notes

(1) (a) Bergbreiter, D. E.; Osburn, P. L.; Wilson, A.; Sink, E. M. *J. Am. Chem. Soc.* **2000**, *122*, 9058. (b) Hamamoto, H.; Suzuki, Y.; Yamada, Y.; Tabata, H.; Takahashi, H.; Ikegami, S. *Angew. Chem., Int. Ed.* **2005**, *44*, 4536.

(2) (a) Uchiyama, S.; Kawai, N.; de Silva, A. P.; Iwai, K. *J. Am. Chem. Soc.* **2004**, *126*, 3032. (b) Hu, Z. B.; Chen, Y. Y.; Wang, C. J.; Zheng, Y. D.; Li, Y. *Nature (London)* **1998**, *393*, 149.

(3) (a) Kanazawa, H.; Yamamoto, K.; Matsushima, Y.; Takai, N.; Kikuchi, A.; Sakurai, Y.; Okano, T. *Anal. Chem.* **1996**, *68*, 100. (b) Kikuchi, A.; Okano, T. *Prog. Polym. Sci.* **2002**, *27*, 1165.

(4) (a) Stayton, P. S.; Shimoboji, T.; Long, C.; Chilkoti, A.; Chen, G.; Harris, J. M.; Hoffman, A. S. *Nature (London)* **1995**, *378*, 472. (b) Matsukata, M.; Aoki, T.; Sanui, K.; Ogata, N.; Kikuchi, A.; Sakurai, Y.; Okano, T. *Bioconjugate Chem.* **1996**, *7*, 96. (c) Ding, Z.; Chen, G.; Hoffman, A. S. *J. Biomed. Mater. Res.* **1998**, *39*, 498.

(5) (a) Yoshida, R.; Sakai, T.; Okano, T.; Sakurai, Y.; Bae, Y. H.; Kim, S. W. *J. Biomater. Sci., Polym. Ed.* **1991**, *3*, 155. (b) Cammas, S.; Suzuki, K.; Sone, Y.; Kakurai, Y.; Kataoka, K.; Okano, T. *J. Controlled Release* **1997**, *48*, 157. (c) Kono, K. *Adv. Drug. Deliv. Rev.* **2001**, *53*, 307.

(6) (a) Park, J. S.; Akiyama, Y.; Winnik, F. M.; Kataoka, K. *Macromolecules* **2004**, *37*, 6786. (b) Diab, C.; Akiyama, Y.; Kataoka, K.; Winnik, F. M. *Macromolecules* **2004**, *37*, 2556.

(7) (a) Kobayashi, S. *Prog. Polym. Sci.* **1990**, *15*, 751. (b) Aoi, K.; Okada, M. *Prog. Polym. Sci.* **1996**, *21*, 151. (c) Kobayashi, S.; Uyama, H. *J. Polym. Sci., Part A: Polym. Chem.* **2002**, *40*, 192.

(8) (a) Heskins, M.; Guillent, J. E.; James, E. J. *J. Macromol. Sci., Chem.* **1968**, *A2*, 1441. (b) Schild, H. G. *Prog. Polym. Sci.* **1992**, *17*, 163.

(9) (a) Woodle, M. C.; Engbers, C. M.; Zalipsky, S. *Bioconjugate Chem.* **1994**, *5*, 493. (b) Zalipsky, S.; Hansen, C. B.; Oaks, J. M.; Allen, T. M. *J. Pharm. Sci.* **1996**, *85*, 133.

(10) (a) Taylor, L. D.; Cerankowski, L. D. *J. Polym. Sci.* **1975**, *13*, 2551. (b) Feil, H.; Bae, Y. H.; Feijen, J.; Kim, S. W. *Macromolecules* **1993**, *26*, 2496.

(11) (a) Sugihara, S.; Kanaoka, S.; Aoshima, S. *Macromolecules* **2004**, *37*, 1711. (b) Ali, M. M.; Stöver, H. D. H. *Macromolecules* **2004**, *37*, 5219. (c) Mori, H.; Iwaya, H.; Nagai, A.; Endo, T. *Chem. Commun.* **2005**, *38*, 4872. (d) Lutz, J.; Hoth, A. *Macromolecules* **2006**, *39*, 893.

(12) (a) Kagiya, T.; Matsuda, T.; Nakato, M.; Hirata, R. *J. Macromol. Sci., Chem.* **1972**, *6*, 1631. (b) Cai, G.; Litt, M. *J. Polym. Sci., Part A: Polym. Chem.* **1992**, *30*, 649. (c) Hoogenboom, R.; Fijten, M. W. M.; Schubert, U. S. *J. Polym. Sci., Part A: Polym. Chem.* **2004**, *42*, 1830.

(13) (a) Pakula, T.; Matyjaszewski, K. *Macromol. Theory Simul.* **1996**, *5*, 987. (b) Matyjaszewski, K.; Ziegler, M. J.; Arehart, S. V.; Greszta, D.; Pakula, T. *J. Phys. Org. Chem.* **2000**, *13*, 775.

(14) Seeliger, W.; Aufderhaar, E.; Diepers, W.; Feinauer, R.; Nehring, R.; Their, W.; Hellmann, H. *Angew. Chem., Int. Ed. Engl.* **1966**, *5*, 875.

(15) Perrin, D. D.; Armarego, W. L. F.; Perrin, D. R. *Purification of Laboratory Chemicals*; Pergamon: Oxford, 1980.

(16) (a) Levy, A.; Litt, M. *J. Polym. Sci., Part A-1* **1968**, *6*, 1883. (b) Litt, M.; Levy, A.; Herz, J. *J. Macromol. Sci., Chem.* **1975**, *A9*, 703. (c) Warakomski, J. M.; Thill, B. P. *J. Polym. Sci., Part A* **1990**, *28*, 3551.

(17) (a) Liu, Q.; Konas, M.; Riffle, J. S. *Macromolecules* **1993**, *26*, 5572. (b) Chen, C. H.; Wilson, J.; Chen, W.; Davis, R. M.; Riffle, J. S. *Polymer* **1994**, *35*, 3587. (c) Kobayashi, S.; Masuda, E.; Shoda, S.; Shimano, Y. *Macromolecules* **1989**, *22*, 2878. (d) Wiesbrock, F.; Hoogenboom, R.; Leenen, M. A. M.; Meier, M. A. R.; Schubert, U. S. *Macromolecules* **2005**, *38*, 5025.

(18) Madruga, E. L. *Prog. Polym. Sci.* **2002**, *27*, 1879.

(19) (a) Saegusa, T.; Ikeda, H.; Fujii, H. *Macromolecules* **1973**, *6*, 315. (b) Saegusa, T.; Kobayashi, S.; Yamada, A. *Makromol. Chem.* **1976**, *177*, 2271. (c) Uyama, H.; Kobayashi, S. *Macromolecules* **1991**, *24*, 614.

(20) Hagipol, C. *Copolymerization-Toward a Systematic Approach*; Kluwer Academic: New York, 1999.

(21) (a) Montaudo, M. S. *Rapid Commun. Mass Spectrom.* **1999**, *13*, 639. (b) Montaudo, M. S. *Mass Spectrom. Rev.* **2002**, *21*, 108.

(22) Terrier, P.; Buchmann, W.; Cheguillaume, G.; Desmazières, B.; Tortajada, J. *Anal. Chem.* **2005**, *77*, 3292.

(23) Lin, P.; Pearce, E. M.; Kwei, T. K. *J. Polym. Sci., Part B: Polym. Phys.* **1988**, *26*, 603.

MA0605548